ASEAN Journal of Science and Engineering

Journal homepage: http://ejournal.upi.edu/index.php/AJSE/

Characteristics of Jengkol Peel (*Pithecellobium jiringa*) Biochar Produced at Various Pyrolysis Temperatures for Enhanced Agricultural Waste Management and Supporting Sustainable Development Goals (SDGs)

*Ali Rahmat[1], Adinda Zahrani[2], Hidayat Hidayat[1], Fera Arum[1], Santi Ari Respati[1], Wiwiek Dwi Susanti[1], Hari Hariadi[1], Abdul Mutolib[3,]**

[1]National Research and Innovation Agency, Indonesia
[2]IPB University, Bogor, Indonesia
[3]Universitas Siliwangi, Tasikmalaya, Indonesia
*Correspondence: E-mail: abdul.mutolib@unsil.ac.id

ABSTRACT

Jengkol peel waste, commonly discarded from households and marketplaces, contributes to environmental pollution due to its lack of nutritional and economic value. Converting this waste into biochar enhances its utility, offering a sustainable solution for waste management. Biochar, rich in carbon, has diverse applications, with its properties significantly influenced by pyrolysis temperature. This study investigates the effect of temperature variations on biochar characteristics. Higher pyrolysis temperatures improved key properties, including pore surface area, total pore volume, fixed carbon content, and mineral composition, particularly phosphorus and magnesium. The most favorable results were obtained at 600°C, where the biochar exhibited optimal porosity, maximum surface area, and the highest fixed carbon content. Additionally, it retained essential macronutrients such as nitrogen, phosphorus, potassium, magnesium, and calcium, making it a promising soil amendment. This research supports sustainable resource utilization and aligns with global sustainability efforts.

ARTICLE INFO

Article History:
Submitted/Received 27 Nov 2024
First Revised 29 Dec 2024
Accepted 27 Feb 2025
First Available online 28 Feb 2025
Publication Date 01 Mar 2025

Keyword:
Biochar,
Biomass,
Characteristics,
Jengkol peel Waste,
Pyrolysis,
Temperature.

1. INTRODUCTION

Pithecellobium jiringa, commonly known as jengkol, represents a significant agricultural resource in Indonesia, with annual production reaching 57,404 tons and showing upward trends. The substantial jengkol production generates considerable biomass waste, particularly shells containing 56.84% lignocellulose content [1]. Studies indicate that jengkol peel waste serves as an economical carbon source [2], and its biochar, combined with organic compost, influences vegetative development [3], suggesting its viability for biochar production.

The accumulation of unutilized jengkol peel waste from markets and households poses environmental concerns, particularly due to sulfuric amino acid decomposition. This situation demands a balanced approach incorporating technological advancement, economic viability, and environmental sustainability [4]. Market-derived jengkol peel, despite its minimal economic worth, presents opportunities as an accessible, cost-effective bio-sorbent from plant materials [5].

One of the effective ways to utilize biomass is by converting it into biochar. Many reports regarding biochar have been well-developed (**Tables 1 and 2**). Biochar applications improve soil moisture retention, potentially strengthening agricultural drought resistance amid climate changes [6]. These applications enhance soil characteristics and fertility by increasing soil carbon and nutrient preservation, subsequently affecting crop productivity [7]. As a soil supplement, biochar's porous structure decreases bulk density, while its nutritional composition enhances soil nutrient accessibility [8-9].

Table 1. Previous studies regarding biochar production from biomass.

No	Title	Ref
1	Development of job sheet application in making biobriquette based on coconut (*Cocos nucifera*) coir with variation of particle size and banana (*Musa paradisica*) peels for vocational students	[10]
2	Influence temperature and holding time of empty fruit bunch slow pyrolysis to phenolic in biocrude oil	[11]
3	Optimal design and techno-economic analysis for corncob particles briquettes: a literature review of the utilization of agricultural waste and analysis calculation	[12]
4	Chemical reaction mechanism from pyrolysis degradation of polystyrene styrofoam plastic microparticles based on FTIR and GC-MS completed with bibliometric literature review to support Sustainable Development Goals (SDGs)	[13]
6	How to calculate and determine chemical kinetics: step-by-step interpretation of experimental data to get reaction rate and order	[14]
7	Valorization of rejected macroalgae *Kappaphycopsis cottonii* for bio-oil and bio-char production via slow pyrolysis	[15]
8	Co-pyrolysis of plastic waste and macroalgae *Ulva lactuca*, a sustainable valorization approach towards the production of bio-oil and biochar	[16]
9	What phenomena happen during pyrolysis of plastic? FTIR and GC-MS analysis of pyrolyzed low linear density polyethylene (LLDPE) polymer particles completed with bibliometric research trend and pyrolysis chemical reaction mechanism	[17]
10	Chemical properties of biochar from date palm seed (*Phoenix dactylifera* L.) under low temperature pyrolysis as soil amendment candidate	[18]
11	Sustainable compost prepared from oyster mushroom substrate microparticles with domestic wastes as local starters	[19]
12	Effect of palm fronds and rice husk composition ratio on the mechanical properties of composite-based brake pad	[20]
13	Chemical properties of salacca seed biochar under low temperature of pyrolysis	[21]
15	Nanocellulose fibers: a review of preparation methods, characterization techniques, and reinforcement applications	[22]

DOI: https://doi.org/10.17509/ajse.v5i1.81297
p- ISSN 2776-6098 e- ISSN 2776-5938

Table 2 (continue). Previous studies regarding biochar production from biomass.

No	Tittle	Ref
16	Fourier Transform Infrared Spectroscopy (FTIR) of pyrolysis of polypropylene microparticles and its chemical reaction mechanism completed with computational bibliometric literature review to Support Sustainable Development Goals (SDGs)	[23]
17	Evaluation of the characteristics of avocado seed biochar at various pyrolysis temperatures for sustainable waste management	[24]
18	Effect of pyrolysis temperature on the properties of biochar derived from melinjo seed shells	[25]
19	Synthesis of carbon microparticles from red dragon fruit (*Hylocereus undatus*) peel waste and their adsorption isotherm characteristics	[26]
20	A review of biomaterial as an adsorbent: From the bibliometric literature review, the definition of dyes and adsorbent, the adsorption phenomena and isotherm models, factors affecting the adsorption process, to the use of typha species waste as a low-cost adsorbent	[27]
21	Investigation of adsorption performance of calcium carbonate microparticles prepared from eggshells waste	[28]
22	Sustainable carbon-based biosorbent particles from papaya seed waste: preparation and adsorption isotherm	[29]
23	A comprehensive study on biochar production, bibliometric analysis, and collaborative teaching practicum for Sustainable Development Goals (SDGs) in islamic schools	[30]
24	Removal of curcumin dyes from aqueous solutions using carbon microparticles from jackfruit seeds by batch adsorption experiment	[31]
25	Adsorption isotherm characteristics of calcium carbon microparticles prepared from chicken bone waste to Support Sustainable Development Goals (SDGs)	[32]
26	Sustainable biochar carbon microparticles based on mangosteen peel as biosorbent for dye removal: theoretical review, modelling, and adsorption isotherm characteristics	[33]
27	Rice husk for adsorbing dyes in wastewater: literature review of agricultural waste adsorbent, preparation of rice husk particles, particle size on adsorption characteristics with mechanism and adsorption isotherm	[34]
28	Sustainable biochar carbon biosorbent based on tamarind (*Tamarindus indica* l) seed: literature review, preparation, and adsorption isotherm	[35]
29	How to purify and experiment with dye adsorption using carbon: step-by-step procedure from carbon conversion from agricultural biomass to concentration measurement using UV Vis spectroscopy	[36]
30	Isotherm and kinetic adsorption of rice husk particles as a model adsorbent for solving issues in the sustainable gold mining environment from mercury leaching	[37]
31	Characteristics of ammonia adsorption on various sizes of calcium carbonate microparticles from chicken eggshell waste	[38]
32	Research trends from the scopus database using keyword water hyacinth and ecosystem: a bibliometric literature review	[39]
33	Progress in the utilization of water hyacinth as effective biomass material	[40]
34	Bibliometrics study on agro-economy of biochar	[41]
35	Bibliometric analysis of the use of biochar in an environmental law perspective	[42]
36	Biochar microparticles from pomegranate peel waste: literature review and experiments in isotherm adsorption of ammonia	[43]
37	Utilizing cassava peel-derived carbon biochar for ammonia adsorption to support hydrogen storage and Sustainable Development Goals (SDGs): effect of microparticle size and isothermal analysis	[44]
38	Red onion peel biomass carbon microparticles for ammonia adsorption for supporting hydrogen storage and Sustainable Development Goals (SDGs) with isotherm analysis	[45]
39	Utilization of orange peel-derived biochar for ammonia adsorption: isotherm analysis and hydrogen storage prospective for supporting Sustainable Development Goals (SDGs)	[46]

In short, the production of biochar involves biomass pyrolysis under oxygen-restricted conditions at temperatures between 400 and 800°C, resulting in a porous, high-pH [47]. Pyrolysis is effective due to its ability to degrade and convert biomass into carbon-related

DOI: https://doi.org/10.17509/ajse.v5i1.81297
p- ISSN 2775-6793 e- ISSN 2775-6815

materials [48-56]. This process benefits agriculture while reducing greenhouse gas emissions [57]. Biochar production decreases as pyrolysis temperatures rise from 400 to 600°C [58], with higher temperatures causing increased degradation of organic materials into ash [59]. Biochars produced at 700°C demonstrate superior soil amendment capabilities [60]. Biochar properties depend on biomass source and carbonization methods [60], influenced by lignin content, mineral levels, particle dimensions, pyrolysis conditions, and pressure [57]. Higher temperatures enhance biochar porosity [61], while pyrolysis temperature affects nutrient composition [62].

Given biochar's potential benefits, investigating jengkol peel biochar characteristics at varying pyrolysis temperatures and its soil amendment efficacy warrants further research. The purpose of this study was to evaluate the characteristics of biochar derived from jengkol peel at different pyrolysis temperatures and to assess its potential as a soil amendment. The novelty of this study lies in exploring the effect of pyrolysis temperature on the physicochemical properties of jengkol peel biochar, which has not been extensively studied. This research provides new insights into optimizing biochar production from agricultural waste, contributing to sustainable waste management and supporting Sustainable Development Goals (SDGs).

2. METHODS

2.1. Feedstock Collection and Preparation

The jengkol (*Pithecellobium jiringa*) peel specimens were collected from a nearby traditional marketplace. These specimens underwent a cleaning process to eliminate dust particles and impurities. Following the cleaning, the material was processed through a chopper and reduced in size until it could pass a 10-mesh screen. Subsequently, the processed specimens underwent drying in an oven at 105°C for 24 h. Once the material cooled to ambient temperature, it was utilized for biochar generation via pyrolysis. The detailed preparation step is shown in **Figure 1**.

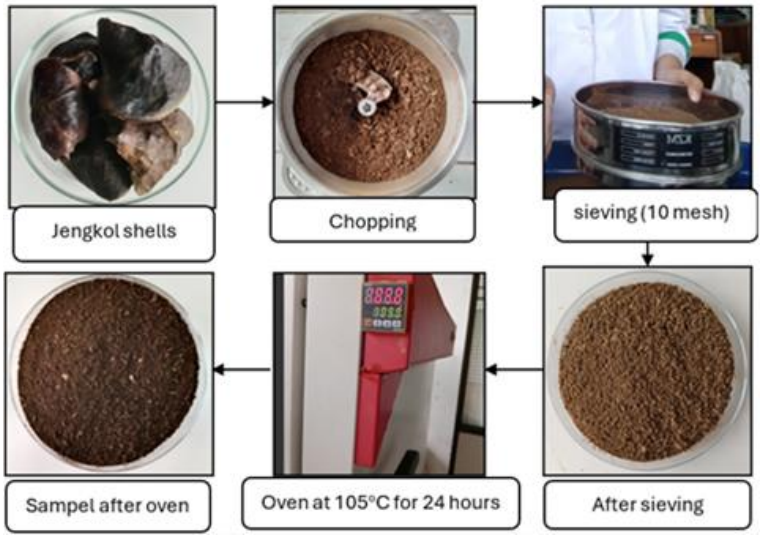

Figure 1. Sample preparation for pyrolysis.

2.2. Biochar Production

A measured sample of jengkol peel (JP) was placed in a 100 mL porcelain cup and covered with aluminum foil to minimize oxygen exposure during the pyrolysis procedure as shown in **Figure 2**. The sample underwent pyrolysis treatment in a Nabertherm L 9/11/SKM muffle

DOI: https://doi.org/10.17509/ajse.v5i1.81297
p- ISSN 2776-6098 e- ISSN 2776-5938

furnace at various temperatures ranging from 300 to 650°C, with 50°C increments. The pyrolysis was maintained for 4 h after temperature stabilization. Following the process, the furnace was deactivated, and the biochar remained at ambient temperature for 24 h to allow complete cooling. Subsequently, the biochar was extracted from the cup, weighed, pulverized, and passed through a 60-mesh sieve in preparation for characterization analysis.

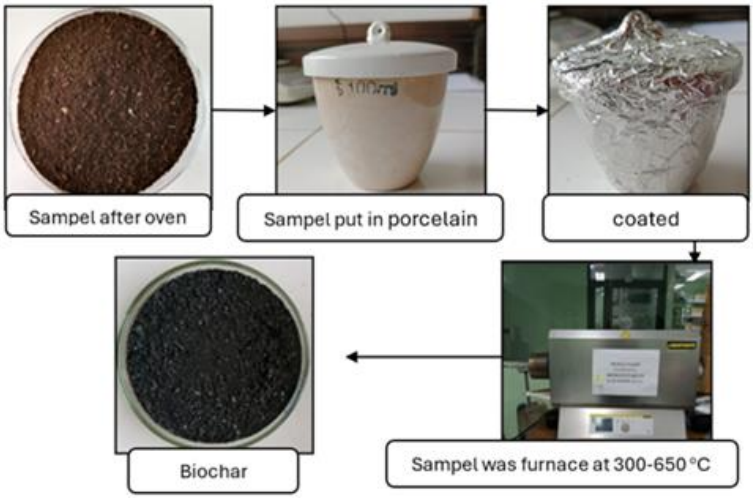

Figure 2. Pyrolysis process.

2.3 Biochar Characterization

The quantity of biochar produced was calculated as a ratio of the final biochar mass to the initial raw material mass. Surface and structural analysis was conducted utilizing FESEM coupled with EDS on a Thermo Scientific Quattro S FESEM instrument. Thermal properties were assessed through TGA and DSC measurements using a NETZSCH STA 449F3 Simultaneous Thermal Analyzer. Crystalline structure evaluation was performed via XRD analysis with a Shimadzu XRD-7000 device. Surface area measurements were obtained through BET analysis using a Quantachrome Nova 4200e analyzer. Chemical bonding and molecular structure were investigated using FTIR-UATR spectroscopy on a Perkin Elmer Spectrum Two instrument.

The compositional characteristics, including moisture, ash, volatile components, and fixed carbon content, were determined through proximate analysis using furnace-based methods. Moisture analysis followed ASTM D3173 protocol, ash content was measured according to ASTM D3174, and the volatile matter was quantified using ASTM D3175. The elemental composition of the jengkol peel biochar was determined using a CHN analyzer, following ASTM D5373 for C, H, and N determination, while S content was measured according to ASTM D4239. K, Mg, and Ca nutrient levels were quantified using a Thermo iCE 3000 series AAS.

3. RESULTS AND DISCUSSION

3.1. Biochar Yield

Jengkol fruit peels underwent pyrolysis across a temperature range of 300°C to 650°C, with biochar yields documented at each temperature point as illustrated in **Figure 3**. The highest yield of 60.46% was observed at 300°C. Subsequently, the yield showed a consistent downward trend with increasing temperatures. The output decreased to 54.14% at 350°C and continued declining to 48.01% at 400°C. Further reductions were observed with yields of 43.38, 41.25, and 38.92% at 450, 500, and 550°C respectively. The lowest yields were recorded at the highest temperatures, with 37.83% at 600°C and 36.63% at 650°C. This inverse relationship between pyrolysis temperature and biochar yield from jengkol peel indicates that

DOI: https://doi.org/10.17509/ajse.v5i1.81297
p- ISSN 2775-6793 e- ISSN 2775-6815

lower temperatures generate greater quantities of biochar.

This finding corresponds with previous research on biochar production from various biomass materials. Biochar production typically decreases with elevated pyrolysis temperatures due to enhanced thermal decomposition of the biomass [63]. Similar findings in studies using safflower seed press cake, where biochar yield decreased as pyrolysis temperature increased [64]. Moreover, reduced biochar production at higher pyrolysis temperatures across different feedstocks, explaining this phenomenon through the progressive release of volatile materials and biomass-to-carbon conversion at elevated temperatures [65].

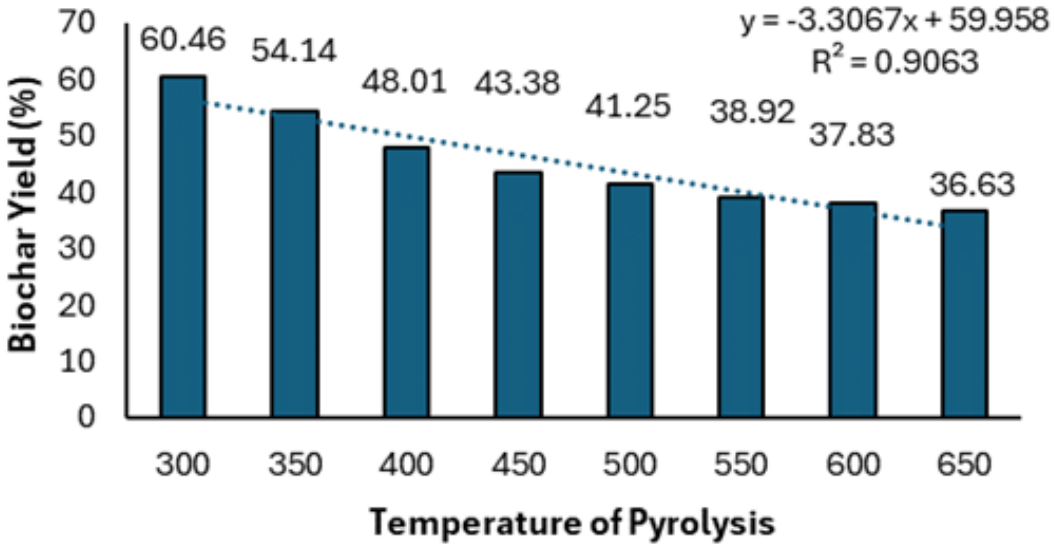

Figure 3. Jengkol peel biochar yields produced in different pyrolysis temperatures.

3.2. Thermogravimetric analysis and Differential scanning calorimetry

Thermogravimetric analysis was employed to investigate the thermal stability and decomposition behavior of biochar samples from the jengkol peel. **Figure 4** shows the TGA curves for the samples pyrolyzed at different temperatures, from 300 to 650°C. Detailed information for the TG-DTA analysis is shown elsewhere [66-67].

The thermogravimetric analysis of JP300 reveals a broad peak around 350°C, signifying substantial mass reduction attributed to organic matter decomposition and functional group volatilization within the biochar structure. For JP350, the TGA curve exhibits a peak shift to higher temperatures, with maximum mass loss near 400°C, reflecting enhanced thermal resistance due to the progressive removal of volatile elements during pyrolysis.

JP400 and JP450 samples display continued peak shifts toward higher temperatures, demonstrating increased thermal stability correlated with elevated pyrolysis temperatures. The diminishing peak intensities suggest decreased volatile content. JP500 and JP550 TGA profiles reveal multiple mass loss events, with a primary peak at approximately 500°C and a secondary feature near 300°C, reflecting the presence of thermally distinct functional groups and carbon structures.

The JP600 sample exhibits a single pronounced peak near 550°C, indicating a primary mass loss event with relatively low intensity, suggesting minimal volatile content. JP650 demonstrates a wide, muted peak maximizing around 600°C, indicating gradual mass reduction across a broader temperature range, characteristic of highly thermally stable materials with minimal volatile components. These DT-TGA curve variations reflect the

DOI: https://doi.org/10.17509/ajse.v5i1.81297
p- ISSN 2776-6098 e- ISSN 2776-5938

systematic removal of volatile matter and the development of heat-resistant carbon structures at increasing pyrolysis temperatures, leading to enhanced thermal stability [68].

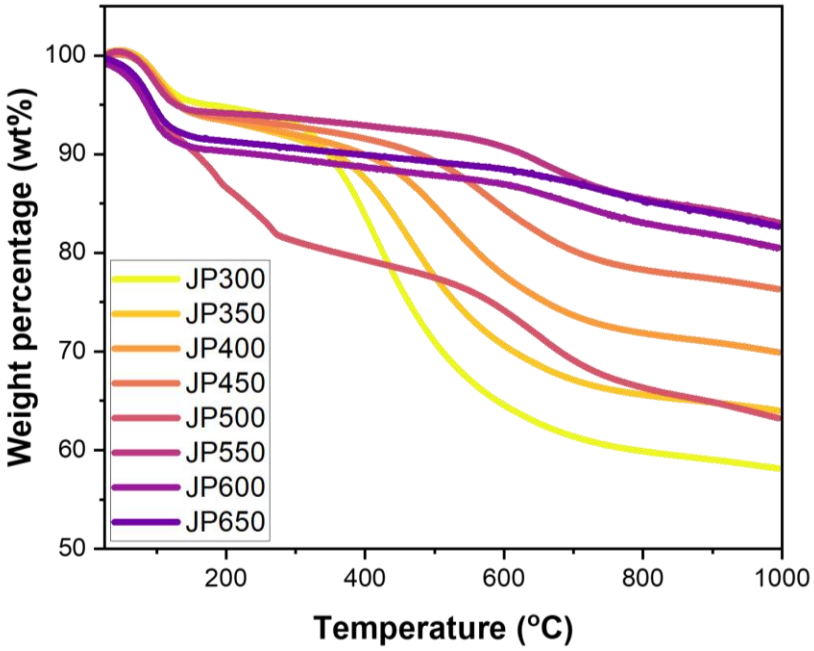

Figure 4. TGA curve for each biochar produced in different temperatures. Note: JP300= biochar produced at 300°C, JP350= biochar produced at 350°C, JP400= biochar produced at 400°C, JP450= biochar produced at 450°C, JP500= biochar produced at 500°C, JP550= biochar produced at 550°C, JP600= biochar produced at 600°C, JP650= biochar produced at 650°C.

DSC analysis of jengkol peel biochar samples produced at temperatures between 300 and 650°C revealed distinctive thermal characteristics (**Figure 5**). All samples displayed a broad endothermic peak below 100°C, associated with moisture evaporation and volatile compound release [69]. A notable exothermic peak emerged between 300 and 500°C, corresponding to carbonaceous material oxidation [47]. These thermal profiles provided crucial information about the samples' structural and chemical transformation [70].

The exothermic peak's location and strength showed significant differences based on the temperature used during biochar formation through pyrolysis. Biochars generated at temperatures between 300 and 400°C displayed more prominent exothermic peaks at lower temperatures, indicating enhanced reactivity and decreased thermal stability. However, when pyrolysis temperatures were elevated (450 to 650°C), the exothermic peak became more focused and shifted to higher temperatures, demonstrating enhanced thermal stability and diminished reactivity [71].

The distinct patterns in DSC curves can be linked to alterations in the biochar samples' chemical makeup and structural characteristics, which were influenced by varying pyrolysis temperatures [72]. Higher pyrolysis temperatures lead to a more complete thermal breakdown and carbonization of the biomass, generating biochars with superior thermal stability and reduced reactivity. Furthermore, as shown in **Figure 4**, the biochar yield percentage demonstrated an inverse relationship with pyrolysis temperature. The highest yield of 60.46% was recorded at 300°C, steadily decreasing to 36.63% when the temperature reached 650°C. This trend highlights the complex connection between pyrolysis temperature and the quantity of biochar produced from jengkol peel source material.

DOI: https://doi.org/10.17509/ajse.v5i1.81297
p- ISSN 2775-6793 e- ISSN 2775-6815

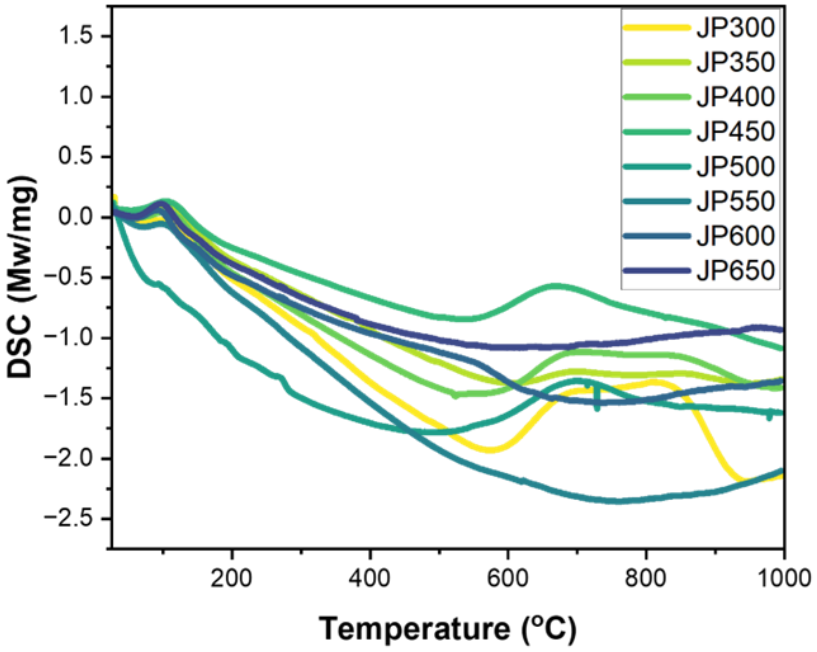

Figure 5. DSC curve for Jengkol peel-based biochar under different pyrolysis temperatures. Note: JP300= biochar produced at 300°C, JP350= biochar produced at 350°C, JP400= biochar produced at 400°C, JP450= biochar produced at 450°C, JP500= biochar produced at 500°C, JP550= biochar produced at 550°C, JP600= biochar produced at 600°C, JP650= biochar produced at 650°C.

3.3. BET Surface of Biochar

BET analysis results demonstrate the surface area, total pore volume, and average pore radius characteristics of the biochar samples. **Table 3** presents comprehensive data for jengkol peel biochar synthesized across various pyrolysis temperatures (300-650°C). The jengkol peel biochar specimens exhibit consistent patterns regarding their BET surface area and total pore volume measurements. As pyrolysis temperatures escalate, the biochar's BET surface area expands correspondingly. The total pore volume demonstrates a positive correlation with increasing pyrolysis temperatures. However, the biochar's average pore radius exhibits an inverse relationship, diminishing progressively as pyrolysis temperatures rise. Detailed information for the BET analysis is shown elsewhere [73].

The BET surface area measurements varied between 4.393 and 149.422 m^2/g across all samples. Minimal BET surface area changes were observed at pyrolysis temperatures between 300 and 500°C. However, significant increases to 61.411 and 149.422 m^2/g occurred at 550 and 600°C, respectively. These elevated BET surface areas at 550 and 650°C likely resulted from intense reactions generating mesoporous structures in the biochar [62]. Pore formation and increased BET surface area occur due to volatile organic component degradation in jengkol peel biochar. Enhanced BET surface area correlates with improved water absorption and soil quality enhancement capabilities. Limited surface area restricts the material's capacity to absorb water and soil nutrients [52].

Pyrolysis temperature elevation corresponds with increased total pore volume in jengkol peel biochar. Higher pyrolysis temperatures facilitate volatile material removal, resulting in expanded micropore volume [62,74]. The total pore volume measured 2.181 x 10^{-2} cc/g at 300°C, reaching its peak of 9.216 x 10^{-2} cc/g at 600°C. Pore boundary wall deformation likely contributes to this volume increase [75]. Elevated pyrolysis temperatures facilitate pore expansion through volatile organic material release [76]. However, at 650°C, both surface

DOI: https://doi.org/10.17509/ajse.v5i1.81297
p- ISSN 2776-6098 e- ISSN 2776-5938

area and total pore volume decreased, attributed to particle surface deterioration as evidenced in morphological analysis.

Table 3. BET surface area analysis of jengkol peel biochar with variations in pyrolysis temperature.

Sample	BET surface area (m^2 /g)	Total Pore Volume x 10^{-2} (cc/g)	Average Pore Radius (nm)
JP 300	4.393	2.181	9.92836
JP 350	6.608	2.772	8.39144
JP 400	5.026	2.108	8.38613
JP 450	10.742	3.209	5.97509
JP 500	5.353	2.623	9.79805
JP 550	61.411	7.303	2.37828
JP 600	149.422	9.216	1.23353
JP 650	27.486	4.932	3.58862

Increased surface porosity correlates with decreased pore radius, as demonstrated by BET analysis results in **Table 3**. The 300°C biochar exhibited the largest average pore radius of 9.92836 nm with minimal surface area. Progressive temperature increases led to smaller pore radii alongside expanded surface area and pore quantity. Pore radii measurements at 350, 400, 450, 500, 550, 600, and 650°C were 8.39144, 8.38613, 5.97509, 9.79805, 2.37828, 1.23353, and 3.58862 nm, respectively. This porous structure enhances biochar's soil improvement capabilities by facilitating root movement and microbial habitat formation.

The porous structure of jengkol peel-derived biochar was investigated using nitrogen adsorption-desorption isotherms at 77 K. The BET isotherms were analyzed for samples treated at temperatures between 300 and 650°C, as shown in **Figure 6**. For specimens JP300, JP350, JP400, and JP450 as shown in **Figures 6A-D**, the BET isotherms revealed Type I characteristics based on IUPAC classification, signifying microporous material composition. A significant increase in adsorption volume was noted at low relative pressures (P/P0 < 0.1), indicating a small micropore presence. The non-overlapping adsorption and desorption paths created a small hysteresis loop, suggesting minimal mesopores or restricted micropores. The microporous network expanded as pyrolysis temperatures increased from 300 to 450°C, with JP450 showing the highest micropore capacity.

Specimens JP500, JP550, JP600, and JP650 exhibited combined Type I and Type IV isotherms as depicted in **Figures 6E-H**, demonstrating both microporous and mesoporous characteristics. Micropore filling was evidenced by swift adsorption at low relative pressures (P/P0 < 0.1), while mesopore capillary condensation produced loops at higher relative pressures (P/P0 > 0.4). JP550 and JP600 demonstrated the most distinct hysteresis loops, indicating well-developed mesoporous structures, with JP600 achieving maximum adsorption volume, suggesting superior surface area and pore capacity. As pyrolysis temperatures increased from 500°C to 650°C, the hysteresis loop diminished, indicating reduced mesoporosity. JP650 showed predominantly Type I behavior with minimal hysteresis, suggesting mainly microporous composition with limited mesopores.

These isotherm changes correlate with the progressive development and subsequent degradation of porous structures during pyrolysis. Micropores predominantly form at temperatures under 450°C, while mesopore formation becomes prominent between 500 and 600°C. At 650°C, mesoporous structures deteriorate, yielding primarily microporous material. These findings demonstrate that jengkol peel biochar's porous characteristics can be

DOI: https://doi.org/10.17509/ajse.v5i1.81297
p- ISSN 2775-6793 e- ISSN 2775-6815

controlled through pyrolysis temperature adjustment, enabling customization for applications requiring specific pore distributions and surface areas.

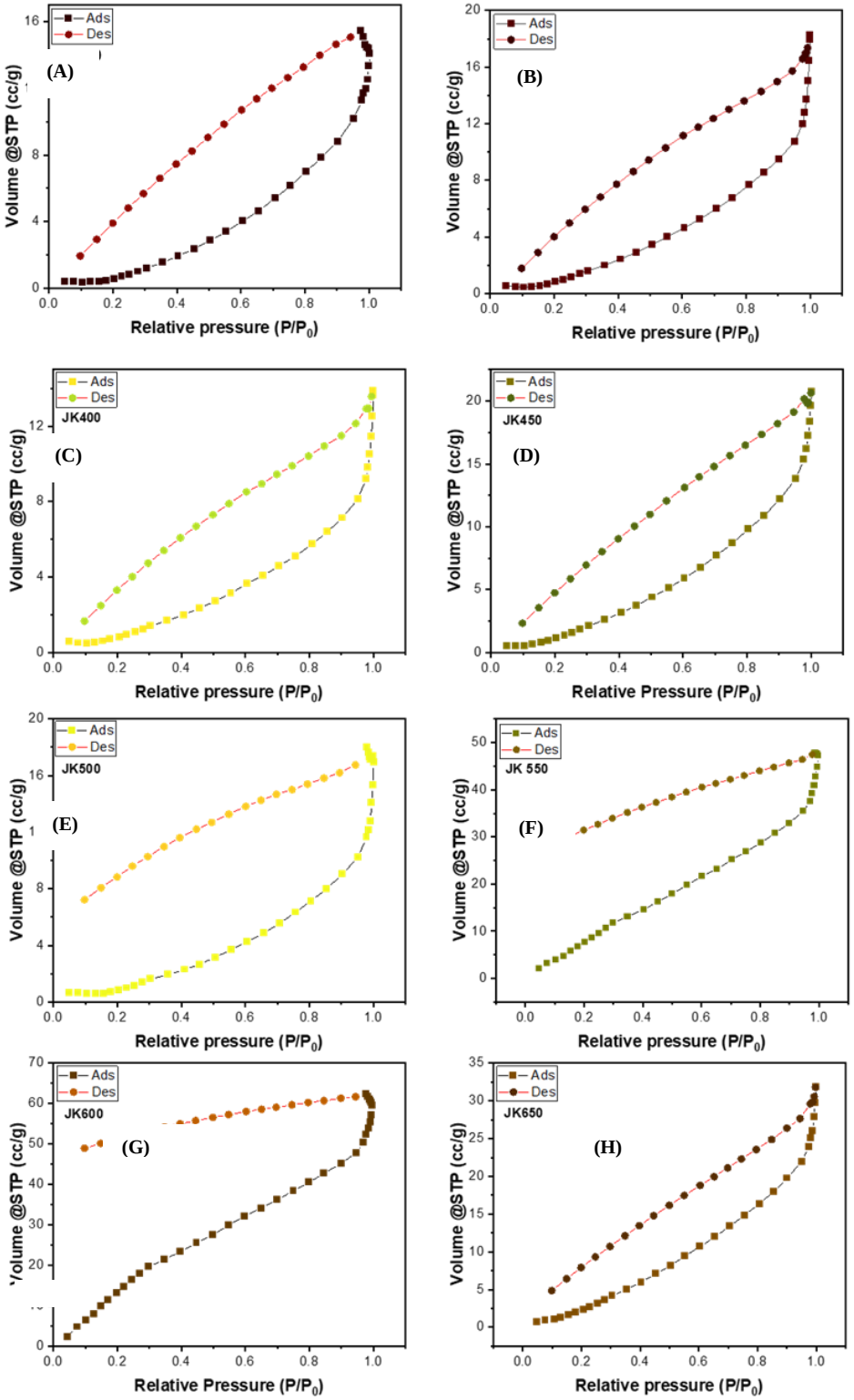

Figure 6. BET curve of (A) JP300, (B) JP350, (C) JP400, (D) JP450, (E) JP500, (F) JP550, (G) JP600, and (H) JP650. Note: JP300= biochar produced at 300°C, JP350= biochar produced at 350°C, JP400= biochar produced at 400°C, JP450= biochar produced at 450°C, JP500= biochar produced at 500°C, JP550= biochar produced at 550°C, JP600= biochar produced at 600°C, JP650= biochar produced at 650°C.

DOI: https://doi.org/10.17509/ajse.v5i1.81297
p- ISSN 2776-6098 e- ISSN 2776-5938

3.4. Morphology of Biochar through SEM Analysis

The morphological characteristics of biochar derived from jengkol peel (*Pithecellobium jiringa*) were investigated using scanning electron microscopy (SEM). The SEM micrographs in **Figure 7** reveal the structural features of samples subjected to pyrolysis at temperatures between 300 and 650°C. Samples JP300, JP350, JP400, and JP450 (**Figures 7A-D**) exhibited irregular and coarse surface characteristics with randomly distributed cavities and void spaces, indicating the development of porosity during activation [77]. The surface irregularity and pore formation became increasingly evident as activation temperatures rose from 300°C to 450°C. The JP450 specimen showed particularly pronounced surface irregularity and permeability, suggesting well-developed microporous features, which aligns with the BET isotherm findings (**Figure 6**).

Specimens JP500, JP550, JP600, and JP650 (**Figures 7E-H**) revealed significant morphological alterations compared to their lower-temperature counterparts. Their surface features displayed increased heterogeneity, incorporating both microscale pores and larger cavities. Notably, JP550 and JP600 specimens demonstrated a structural composition combining both micro and mesopores, which was further supported by the presence of characteristic hysteresis loops in their respective BET isotherms.

The enhanced mesoporosity and surface area in these samples can be attributed to the presence of larger pores and cavities. When pyrolysis reaches 650°C (JP650 sample), the surface structure exhibits increased density and decreased porosity, showing fewer significant pores and voids. This finding corresponds with the diminished hysteresis loop observed in the BET isotherm (**Figure 6**), indicating decreased mesoporosity at higher activation temperatures.

These structural changes result from the progressive development and breakdown of the porous structure during pyrolysis. Micropores predominantly form at temperatures under 450°C. As temperatures rise between 500 and 600°C, mesopore formation becomes more prominent, creating a highly diverse and porous surface structure. At 650°C, the mesoporous framework deteriorates, producing a more condensed, primarily microporous material. The SEM analysis reveals crucial details about the biochar samples' morphological transformations. These findings supplement the BET isotherm data, enabling a comprehensive understanding of both the porous structure and its relationship with activation temperature.

3.5. X-ray Diffraction Analysis of Jengkol Peel Biochar

The X-ray diffraction analysis (**Figure 8**) reveals a prominent and symmetrical primary diffraction peak at lower 2θ angles, indicating mineral crystal formation. Specific peaks observed at 24.4, 28.6, and 40.7° signify the occurrence of CaO, $CaCO_3$, and CaO, respectively. The XRD pattern shows reduced or flattened peaks as the pyrolysis temperature increases, reflecting the progressive crystallization transformation of CaO and $CaCO_3$. Higher pyrolysis temperatures promote inorganic particle precipitation and crystallization development [78]. The jengkol peel's cellulose and lignin components progressively decompose, generating significant ash content. This ash predominantly contains mineral elements, such as silicates, potassium salts, and calcium carbonate.

XRD patterns for solid samples were measured at various temperatures. The biochar created at a pyrolysis temperature of 400°C prominently displayed an identifiable amorphous carbon crystalline phase between approximately 21 and 24°. Conversely, this phase was absent in the biochar derived from pyrolysis at 650°C, suggesting a potential interaction with other inorganic materials in solid form. When heating wet banana peel at temperatures

DOI: https://doi.org/10.17509/ajse.v5i1.81297
p- ISSN 2775-6793 e- ISSN 2775-6815

spanning from 400 to 650°C, biochar's amorphous carbon generally shows broad diffraction peaks, indicative of limited graphitization. This situation is primarily linked to a high ash content, leading to reduced carbon levels, which is unfavourable as it transforms into aromatic compounds during pyrolysis. The biochar's hydrophilicity is chiefly determined by ash levels rather than the pyrolysis approach (**Figure 8**). At a pyrolysis temperature of 300°C, the concentration of inorganic compounds was noticeably lower than at 650°C, resulting in biochar displaying enhanced hydrophobicity [6].

In comparison, the further breakdown of organic content resulted in an increased carbon and inorganic component ratio while diminishing the number of hydrophilic functional groups on the biochar surface. Additionally, the influence of ash on hydrophilicity is markedly stronger than the effects of decreasing hydrophilic functional groups and increasing carbon content. Pre-treating jengkol shells to remove moisture before pyrolysis boosts the decomposition of organic molecules and the release of volatile substances, leading to a higher proportion of ash, which correlates with increased hydrophilicity in the biochar [79]. Turbostratic carbon, characterized by a less orderly structure compared to graphite, possesses several important properties relevant to pyrolysis and biochar production [80].

Increasing the pyrolysis temperatures to 300, 350, 400, 450, 500, 550, 600, and 650°C led to a decrease in the strength and broadening of the jengkol peel cellulose crystal peak (full-width half maximum). This effect results from the volatilization of components within the lignocellulose framework and the lack of lateral connections between polymer chains during pyrolysis. It further contributes to a reduction in polymer chain aggregation [81], facilitating the expansion of the jengkol peel. Particularly, the absence of oxygen and hydrogen atoms causes fragmentation of polymer chains found in cellulose, hemicellulose, and lignin. Free monomer units promote the formation of the amorphous carbon phase consisting of aliphatic chains and aromatic rings, mainly sourced from hemicellulose and lignin. As pyrolysis temperatures increase, the gradual condensation of these aromatic rings leads to the development of interconnected conjugated sheets, eventually resulting in the formation of a turbostratic carbon structure [82].

The dominant peaks of the turbostratic phase can be found at (002) with a 2θ angle of 24.4° and (100) with a 2θ angle of 40.4°. The cellulose and turbostratic phases at a pyrolysis temperature of 400°C demonstrate minimal crystal organization, as shown by JP 300 and JP 350. Beyond 400°C, the turbostratic peak intensity, which reflects both the turbostratic ordered phase and the amorphous phase, increases. Consequently, biochar is characterized as a continuous array of carbon molecules, incorporating both crystalline and amorphous structures. Reflections of the turbostratic (100) phase can be observed in the JP 500 to JP 600 range, with their intensity increasing as the temperature rises, indicating growth in carbon structures and interconnected aromatic sheets during pyrolysis. Within the tested pyrolysis temperature spectrum, the arrangement of aromatic rings resulting from cellulose's thermochemical decomposition enhances the lateral growth of graphene-like layers. Interestingly, the (002) reflection strength, which indicates the presence of the aromatic layer of the turbostratic phase along the z-axis, appears unaffected by its lateral expansion [83]. At pyrolysis temperatures of 500 and 650°C, a decrease in the intensity of the (002) peak for the jengkol shell hints at a slight reduction in the spacing between graphene-like sheets along the z-axis. This decrease could be attributed to the presence of additional carbon atoms in the dense amorphous biochar matrix. Biochar exhibits a turbostratic structure and features unique characteristics that render it suitable for a variety of applications, such as energy storage (batteries, supercapacitors), filtration, and adsorption. These distinctive properties stem from the carbon framework of the biochar [84-85].

DOI: https://doi.org/10.17509/ajse.v5i1.81297
p- ISSN 2776-6098 e- ISSN 2776-5938

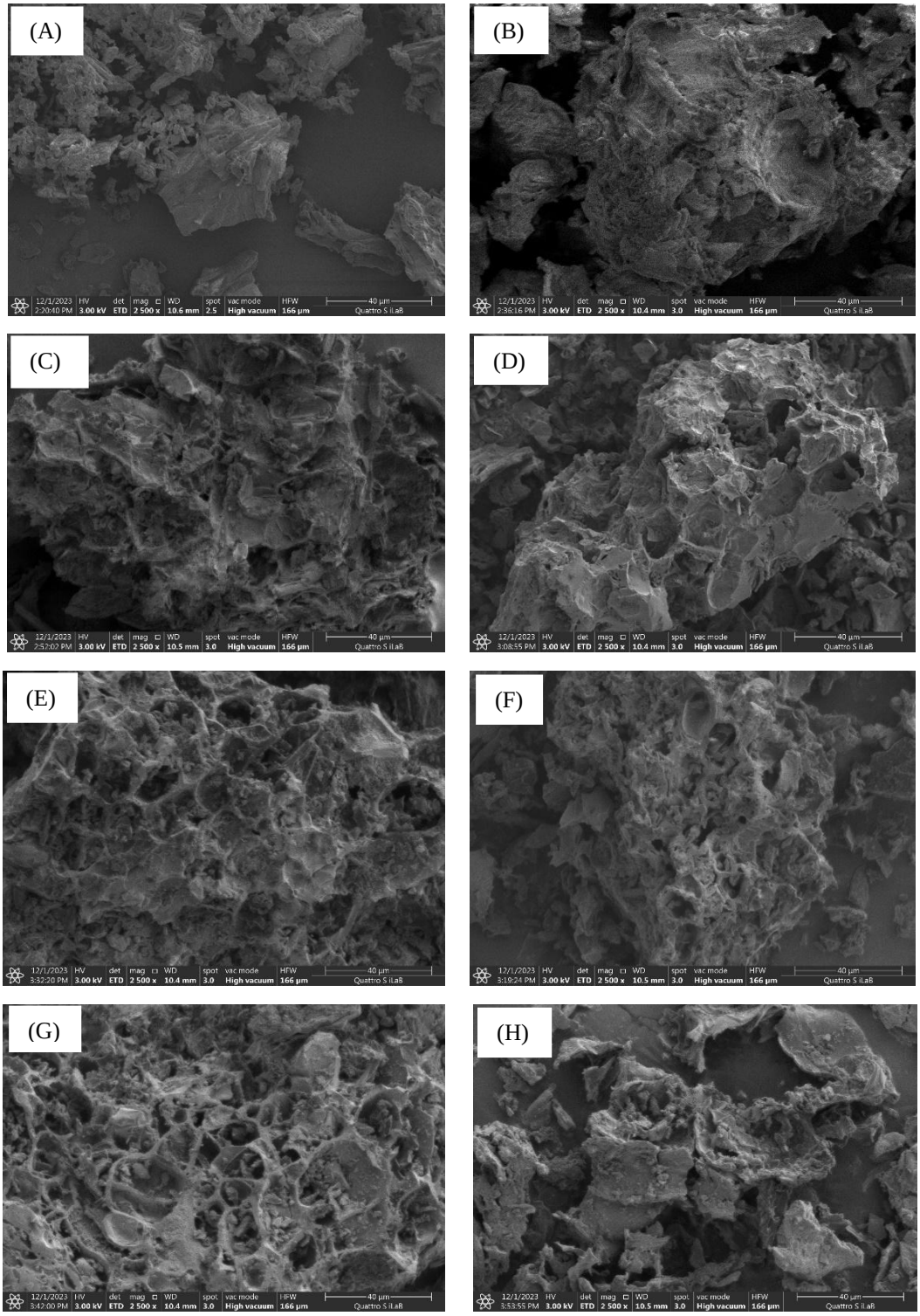

Figure 7. Morphology of (A) JP300, (B) JP350, (C) JP400, (D) JP450, (E) JP500, (F) JP550, (G) JP600, and (H) JP650. Note: JP300= biochar produced at 300°C, JP350= biochar produced at 350°C, JP400= biochar produced at 400°C, JP450= biochar produced at 450°C, JP500= biochar produced at 500°C, JP550= biochar produced at 550°C, JP600= biochar produced at 600°C, JP650= biochar produced at 650°C.

DOI: https://doi.org/10.17509/ajse.v5i1.81297
p- ISSN 2775-6793 e- ISSN 2775-6815

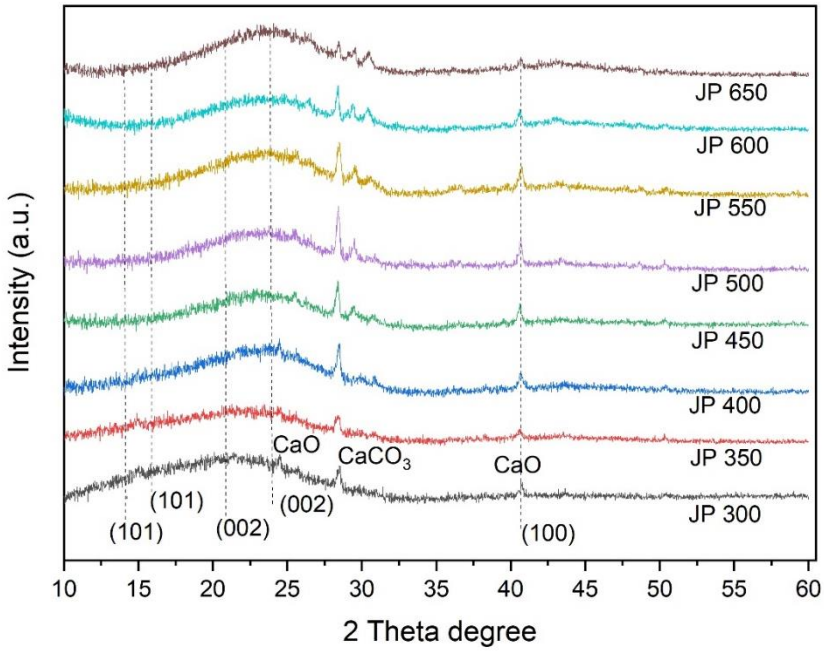

Figure 8. XRD of jengkol peel biochar. Note: JP300= biochar produced at 300°C, JP350= biochar produced at 350°C, JP400= biochar produced at 400°C, JP450= biochar produced at 450°C, JP500= biochar produced at 500°C, JP550= biochar produced at 550°C, JP600= biochar produced at 600°C, JP650= biochar produced at 650°C.

3.6. FTIR of Jengkol Peel Biochar

Within the jengkol peel's structure, various functional components can be identified (**Figure 9**). Detailed information regarding FTIR is explained elsewhere [86-89]. O-H stretch bonds alongside alcohol and phenol groups detected within the 3500–3200 cm^{-1} vibrational scope. The material demonstrates aliphatic C-H and aromatic C=C stretching movements at 2920 and 1600 cm^{-1} respectively. C-O bond stretching vibrations are evident at 1120 and 1008 cm^{-1}, characteristic of multiple organic substances including alcohols, phenols, acids, ethers, and esters [90]. The peel also shows cellulose-related C-H stretching at 2926 and 1608 cm^{-1}. Evidence of lignin and hemicellulose appears through C=C group stretching vibrations at 1590 cm^{-1}. Supporting these findings are cellulose-based C-H bending vibrations occurring at 1435 and 1395 cm^{-1}. As noted in the literature [91], the 1008 cm^{-1} reading indicates C-O combination activity.

With rising temperatures, the intensity of hydroxyl groups in C-H stretches of aliphatic compounds and the carbonyl C=O signal becomes weaker. The FTIR spectrum shows a notable decrease in O-H stretch vibration at 3500-3200 cm^{-1} during pyrolysis, which results from enhanced dehydration of the jengkol shell. Between 300 and 650°C, aliphatic O-H and C-H functional group absorption intensities weaken, mainly due to cellulose and hemicellulose dehydration and the reduction of aliphatic functionalities in jengkol peel samples [92].

FTIR analysis demonstrates significant changes in characterization results. Hydroxyl group (-OH) absorption strength diminishes at temperatures starting from 300°C and disappears entirely at 650°C. Lignin intensity shows a reduction at lower temperatures but strengthens with temperature elevation. Aromatic rings, generated through lignin's thermal decomposition, constitute the main structure of jengkol peel biochar. The absorption bands in biochar FTIR analysis appear weaker at 650°C compared to 300°C, indicating the conversion of biomass elements (extractives, holocellulose, and lignin) during pyrolysis into residual

DOI: https://doi.org/10.17509/ajse.v5i1.81297
p- ISSN 2776-6098 e- ISSN 2776-5938

biochar components. Carbon decomposition represents the primary pyrolysis reaction [93]. Biochar produced at 300°C exhibits a clear wave number around 1000 cm^{-1}, which undergoes a shift at 650°C. This phenomenon occurs due to the thorough decomposition of cellulose, hemicellulose, and lignin at higher temperatures, generating thermally stable aromatic structures [79,94].

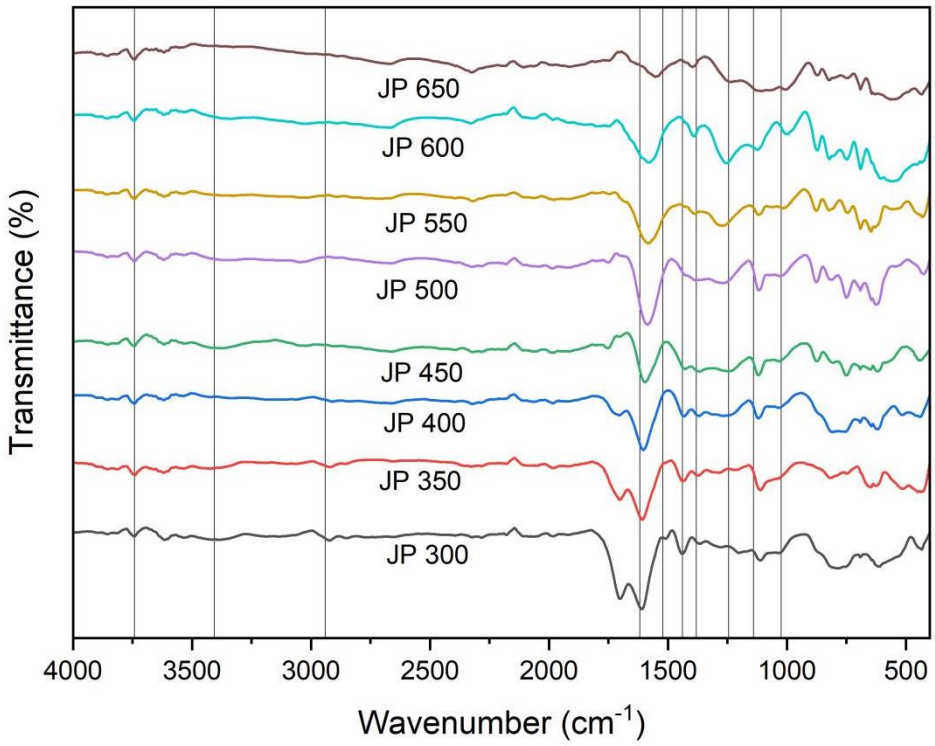

Figure 9. FTIR of jengkol peel biochar. Note: JP300= biochar produced at 300°C, JP350= biochar produced at 350°C, JP400= biochar produced at 400°C, JP450= biochar produced at 450°C, JP500= biochar produced at 500°C, JP550= biochar produced at 550°C, JP600= biochar produced at 600°C, JP650= biochar produced at 650°C.

3.7. Proximate Analysis of Biochar

The proximate analysis findings demonstrate how temperature variations in jengkol peel biochar pyrolysis influence the levels of fixed carbon, volatile matter, ash, and water content, as shown in **Table 3**. The proximate analysis reveals that volatile matter in jengkol peel biochar decreases as pyrolysis temperature rises. Conversely, both fixed carbon and ash demonstrate a positive correlation with increasing pyrolysis temperature. The biochar exhibits a fixed carbon content of 51.66% when pyrolyzed at 300°C, with this percentage progressively increasing at higher temperatures. The maximum fixed carbon content of 77.76% is achieved when the pyrolysis temperature reaches 650°C. These findings align with literature [95], who observed that higher pyrolysis temperatures lead to increased fixed carbon content while simultaneously reducing volatile substances.

Jengkol peel biochar produced at 300°C exhibits a volatile matter content of 38.76%, which progressively diminishes with elevated pyrolysis temperatures. At the maximum pyrolysis temperature of 650°C, the volatile matter reaches its lowest level of 7.37%. This observation aligns with findings from previous studies [96], who demonstrated an inverse relationship between pyrolysis temperature and volatile matter content in biochar. Both the pyrolysis temperature and biochar source material influence the volatile substance levels [97].

DOI: https://doi.org/10.17509/ajse.v5i1.81297
p- ISSN 2775-6793 e- ISSN 2775-6815

Table 3. Proximate analysis of jengkol peel biochar pyrolyzed at various temperatures.

Sample	Fixed carbon (%)	Volatile matter (%)	Ash content (%)	Water conten (%)
JP 300	51.66	38.76	3.90	5.69
JP 350	57.52	32.67	4.40	5.41
JP 400	60.90	28.77	4.84	5.48
JP 450	67.13	22.17	5.44	5.26
JP 500	73.42	15.55	5.82	5.21
JP 550	73.78	13.88	6.82	5.52
JP 600	74.70	11.07	7.76	6.47
JP 650	77.76	7.37	7.18	7.69

The moisture content remains relatively constant at 5% for biochar produced between 300-550°C, but shows an upward trend at higher temperatures, reaching 6% and 7% at 600 and 650°C, respectively. This moisture increase can be attributed to enhanced water vapor absorption due to expanded surface pores at elevated temperatures [98]. Similarly, the ash content demonstrates a positive correlation with pyrolysis temperature. Starting at 3.90% for biochar produced at 300°C, the ash content steadily increases with temperature elevation. This rise in ash content occurs due to the retention of inorganic minerals following the decomposition of carbon, oxygen, and hydrogen elements in the biomass [99]. Elevated ash content is typically considered disadvantageous, as the inorganic mineral components can obstruct internal pores, reducing accessibility to biochar surface sorption sites.

3.8. Ultimate Analysis of Biochar

Ultimate analysis was performed to check the carbon, hydrogen, nitrogen, sulfur, and oxygen content in jengkol peel biochar. The ultimate analysis of jengkol peel biochar results is shown in **Table 4**.

Table 4. Ultimate analysis of jengkol peel biochar pyrolyzed with temperature variations.

Sample	Carbon (%)	Hydrogen (%)	Nitrogen (%)	Sulfur (%)	Oxygen (%)
JP 300	63.51	4.80	3.59	0.34	23.87
JP 350	65.78	4.39	3.22	0.27	21.94
JP 400	69.30	3.90	2.76	0.20	19.00
JP 450	72.53	3.57	2.74	0.21	15.52
JP 500	74.00	3.18	2.58	0.19	14.25
JP 550	75.46	2.98	3.20	0.39	11.16
JP 600	74.49	2.60	2.96	0.34	11.86
JP 650	73.32	2.24	2.81	0.29	14.16

The pyrolysis temperature exhibits a positive correlation with the carbon concentration in jengkol peel biochar. Starting at 63.51% carbon content at 300°C, the biochar shows progressive increases with temperature elevation, reaching 75.46% at 550°C. This elevated carbon composition allows biochar to function effectively as a carbon reservoir, serving both as an energy resource and soil contaminant absorbent [97]. The carbon-rich biochar demonstrates long-term stability in soil environments and contributes to both soil enhancement and global CO_2 reduction.

Conversely, higher pyrolysis temperatures lead to decreasing hydrogen and oxygen levels in jengkol peel biochar. Hydrogen content peaks at 4.80% when pyrolyzed at 300°C but diminishes to 2.24% at 650°C. Similarly, oxygen levels decline from 23.87% at 300°C to 14.16% at 650°C. Enhanced carbonification occurs at higher pyrolysis temperatures, resulting in

DOI: https://doi.org/10.17509/ajse.v5i1.81297
p- ISSN 2776-6098 e- ISSN 2776-5938

increased carbon levels while reducing hydrogen and oxygen content [100]. Some reports [101] attribute this reduction to the breakdown of less stable bonds within the biochar structure, yielding a predominantly carbon-based material at elevated temperatures.

The nitrogen composition of jengkol peel biochar also shows an inverse relationship with pyrolysis temperature. The maximum nitrogen content of 3.59% observed at 300°C gradually reduces to 2.81% at 650°C. This reduction is likely attributed to ammonia volatilization and the release of nitrogen-containing organic compounds during pyrolysis. Sulfur levels remain consistently low across all temperature treatments, reflecting the minimal sulfur content in the original material. The sulfur percentage decreases from 0.34 to 0.19% as temperatures rise from 300 to 500°C. This reduction is primarily due to element volatilization during pyrolysis, predominantly in the form of carbonyl sulfide [102].

3.9. Nutrient Content of Jengkol Peel Biochar

Nutrient content analysis of jengkol peel biochar was conducted to quantify nutritional constituents at varying pyrolysis temperatures. The relationship between pyrolysis temperature and nutrient composition was determined using AAS thermo iCE 3000 series analysis, with results presented in **Table 5**.

Table 5. Nutrient content in jengkol peel biochar at various pyrolysis temperatures.

Sample	N-total (mg/g)	Phosphor (P) (mg/g)	Kalium (K) (mg/g)	Magnesium (Mg) (mg/g)	Calcium (Ca) (mg/g)
JP 300	7.55	1.42	3.75	1.37	1.01
JP 350	8.46	1.25	3.38	1.94	1.65
JP 400	9.01	1.82	3.94	2.55	2.13
JP 450	8.35	2.66	3.51	3.55	1.66
JP 500	8.49	2.84	3.99	4.48	1.10
JP 550	8.24	2.54	4.08	5.69	1.74
JP 600	8.30	2.66	3.55	6.09	0.88
JP 650	7.98	2.55	3.83	6.22	0.78

The analysis of jengkol peel biochar pyrolyzed between 300 and 650°C revealed stable total nitrogen content, showing minimal variation. The nitrogen levels ranged from 7.55 mg/g at 300°C to 7.98 mg/g at 650°C, with a peak content of 9.01 mg/g occurring at 400°C. When introduced to soil, biochar's nitrogen content supports plant growth through enhanced chlorophyll formation, amino acid production, and protein synthesis [103].

The biochar's phosphorus levels exhibited an upward trend with increasing pyrolysis temperatures. Samples processed at 300, 350, and 400°C contained 1.42, 1.25, and 1.82 mg/g of phosphorus respectively, rising to 2 mg/g at temperatures between 450 and 650°C. Plants benefit from phosphorus through improved photosynthesis, respiration, energy processes, cellular growth, and root development [104].

Potassium content remained relatively constant across different pyrolysis temperatures, with values ranging from a peak of 4.08 mg/g at 550°C to a minimum of 3.38 mg/g at 350°C. This consistency stems from potassium's thermal stability. Biochar's potassium becomes available in soil solution, facilitating plant absorption while reducing leaching [105]. Potassium supports various plant functions, including root growth, protein formation, disease resistance, and seed development [106].

Magnesium concentrations showed consistent increases with higher pyrolysis temperatures, reaching a maximum of 6.22 mg/g at 650°C. This trend results from magnesium's resistance to evaporative loss during pyrolysis [107]. As a component of ash

DOI: https://doi.org/10.17509/ajse.v5i1.81297
p- ISSN 2775-6793 e- ISSN 2775-6815

[98], magnesium levels rise correspondingly with increasing ash content through organic material decomposition at higher temperatures.

As a crucial secondary macronutrient for plant development, calcium has been extensively studied [108]. In jengkol peel biochar, calcium content initially increased from 300 to 400°C, peaking at 2.130 mg/g, before declining to 0.788 mg/g at 650°C. The calcium levels showed irregular fluctuations with increasing temperatures, generally maintaining low, stable concentrations between 300 and 650°C, likely due to temperature-related retention properties and limited initial calcium content in the source material.

3.10. Contribution to Sustainable Development Goals (SDGs)

The conversion of jengkol (*Pithecellobium jiringa*) peel waste into biochar plays a significant role in advancing multiple Sustainable Development Goals (SDGs) by addressing environmental sustainability, agricultural productivity, and educational development. This approach aligns with SDG 12 (Responsible Consumption and Production) by minimizing agricultural waste disposal in landfills and promoting a circular economy through resource reutilization.

A practical example comes from field trials in Palembang, Indonesia, where the application of jengkol peel biochar (15 tons/ha) combined with chicken manure (30 tons/ha) resulted in a red chili yield of 10.99 tons/ha. This demonstrates a direct contribution to SDG 2 (Zero Hunger) by enhancing soil fertility and crop productivity, particularly in acidic drylands [109]. The biochar's porous nature aids in nutrient retention and water conservation, thereby mitigating soil degradation and supporting SDG 15 (Life on Land) [110]. Furthermore, the pyrolysis process not only generates syngas as a renewable energy source, aligning with SDG 7 (Affordable and Clean Energy), but also facilitates long-term carbon sequestration in the soil, contributing to SDG 13 (Climate Action) by lowering atmospheric CO_2 levels [110,111].

Beyond its environmental impact, this biochar valorization initiative also fosters SDG 4 (Quality Education) by integrating hands-on learning opportunities into school curricula. Islamic boarding schools, for instance, have incorporated biochar production training, enabling students to gain practical experience in sustainable agriculture and environmental conservation [30]. Additionally, collaborations between agricultural and educational institutions illustrate SDG 17 (Partnerships for the Goals), reinforcing the connection between scientific research and community-driven solutions.

By transforming agricultural waste into a valuable resource, this strategy presents a cost-effective and scalable solution to advancing multiple SDGs while simultaneously addressing local agricultural and ecological challenges.

4. CONCLUSION

The properties of jengkol peel biochar improve with increasing pyrolysis temperature, enhancing its pore structure, fixed carbon content, and essential minerals like phosphorus and magnesium. At higher temperatures, the biochar develops an optimal porous structure, improving nutrient retention and soil enrichment, making it a promising soil amendment.

Additionally, this approach supports sustainability by repurposing agricultural waste and enhancing soil productivity, contributing to responsible resource use. By converting waste into a valuable resource, this strategy offers a cost-effective and scalable solution to agricultural and environmental challenges.

DOI: https://doi.org/10.17509/ajse.v5i1.81297
p- ISSN 2776-6098 e- ISSN 2776-5938

5. AUTHORS' NOTE

The authors declare that there is no conflict of interest regarding the publication of this article. Authors confirmed that the paper was free of plagiarism.

6. REFERENCES

[1] Sari, F. I. P., and Asriza, R. O. (2018). Biosorben kulit jengkol sebagai penyerap logam Pb pada air kolong pasca penambangan timah. *Jurnal Sains Teknologi dan Lingkungan, 4(2),* 83-89.

[2] Taer, E., and Taslim, R. (2021). The effect of physical activation temperature on physical and electrochemical properties of carbon electrode made from jengkol shell (*Pithecellobium jiringa*) for supercapacitor application. *Materials Today: Proceedings, 44*, 3341-3345.

[3] Hasibuan, N. M., Hutapea, S., and Rahman, A. (2022). Utilization of jengkol skin waste as an ingredient to increase the growth and production of shallot (*Allium ascalonicum* L.). *Ilmiah Pertanian (JIPERTA) Journal, 4*(1), 32-44.

[4] Prayugo, A. S., Gea, S., Daulay, A., Harahap, M., Siow, J., Goei, R., and Tok, A. I. Y. (2023). Highly fluorescent nitrogen-doped carbon dots derived from jengkol peels (*Archindendron pauciflorum*) by solvothermal synthesis for sensitive Hg^{2+} ions detection. *Biosensors and Bioelectronics: X, 14*, 100363.

[5] Rezić, I. (2013). Cellulosic fibers—Biosorptive materials and indicators of heavy metals pollution. *Microchemical Journal, 107*, 63-69.

[6] Edeh, I. G., and Mašek, O. (2022). The role of biochar particle size and hydrophobicity in improving soil hydraulic properties. *European Journal of Soil Science, 73*(1), e13138.

[7] Mullen, C. A., Boateng, A. A., Goldberg, N. M., Lima, I. M., Laird, D. A., and Hicks, K. B. (2010). Bio-oil and biochar production from corn cobs and stover by fast pyrolysis. *Biomass and Bioenergy, 34*, 67-74.

[8] Ashworth, A. J., Sadaka, S., Allen, F. L., Sharara, M. A., and Keyser, P. D. (2014). Influence of pyrolysis temperature and production conditions on switchgrass biochar for use as a soil amendment. *BioResources, 9*(4), 7622-7635.

[9] Luo, Y., Durenkamp, M., De Nobili, M., Lin, Q., and Brookes, P. C. (2011). Short-term soil priming effects and the mineralisation of biochar following its incorporation to soils of different pH. *Soil Biology and Biochemistry, 43*(11), 2304-2314.

[10] Nandiyanto, A. B. D., Rachmat, L. A., Rahayu, D. L., Azizah, N. N., and Husaeni, D. F. A. (2020). Development of Job sheet Application in Making Biobriquette Based on Coconut (*Cocos nucifera*) Coir with Variation of Particle Size and Banana (*Musa paradisica*) Peels for Vocational Students. *Journal of Engineering Education Transformations, 34*(Special Issue), 132-138.

[11] Irawan, A., Kurniawan, T., Alwan, H., Darisman, D., Pujianti, D., Bindar, Y., Abu Bakar, M. S., and Nandiyanto, A. B. D. (2021). Influence of temperature and holding time of

DOI: https://doi.org/10.17509/ajse.v5i1.81297
p- ISSN 2775-6793 e- ISSN 2775-6815

empty fruit bunch slow pyrolysis to phenolic in biocrude oil. *Automotive Experiences, 4*(3), 150-160.

[12] Nandiyanto, A. B. D., Azizah, N. N., and Girsang, G. C. S. (2022). Optimal design and techno-economic analysis for corncob particles briquettes: A literature review of the utilization of agricultural waste and analysis calculation. *Applied Science and Engineering Progress*, *15*(3), 5508-5508.

[13] Nandiyanto, A. B. D., Kaniawati, I., Kurniawan, T., Farobie, O., and Bilad, M. R. (2024). Chemical reaction mechanism from pyrolysis degradation of polystyrene styrofoam plastic microparticles based on FTIR and GC-MS completed with bibliometric literature review to support sustainable development goals (SDGs). *Moroccan Journal of Chemistry*, *12*(3), 1380-1398.

[14] Nandiyanto, A. B. D., Ragadhita, R., and Fiandini, M. How to calculate and determine chemical kinetics: Step-by-step interpretation of experimental data to get reaction rate and order. *Indonesian Journal of Science and Technology*, *9*(3), 759-774.

[15] Farobie, O., Amrullah, A., Syaftika, N., Bayu, A., Hartulistiyoso, E., Fatriasari, W., and Nandiyanto, A. B. D. (2024). Valorization of rejected macroalgae *Kappaphycopsis cottonii* for bio-oil and bio-char production via slow pyrolysis. *ACS Omega*, *9*(14), 16665-16675.

[16] Farobie, O., Amrullah, A., Fatriasari, W., Nandiyanto, A. B. D., Ernawati, L., Karnjanakom, S., Lee, S. H., Selvasembian, R., Wan Azelee, N. I., and Aziz, M. (2024). Co-pyrolysis of plastic waste and macroalgae *Ulva lactuca*, a sustainable valorization approach towards the production of bio-oil and biochar. *Results in Engineering, 24*, 103098.

[17] Nandiyanto, A. B. D., Sucianto, R. N., Matildha, S. R., Nur, F. Z., Kaniawati, I., Kurniawan, T., Bilad, M. R., and Che Sidik, N. A. (2025). What phenomena happen during pyrolysis of plastic? FTIR and GC-MS analysis of pyrolyzed low linear density polyethylene (LLDPE) polymer particles completed with bibliometric research trend and pyrolysis chemical reaction mechanism. *Journal of Advanced Research in Applied Sciences and Engineering Technology, 46*(1), 250-260.

[18] Rahmat, A. (2021). Chemical properties of biochar from date palm seed (Phoenix dactylifera L.) under low temperature pyrolysis as soil amendment candidate. *Applied Research in Science and Technology*, *1*(2), 116-120.

[19] Rahmat, A., Ramadhani, W. S., Hidayat, H., Kurniawan, K., Hariadi, H., Nuraini, L., Iresha, F. M., Nurtanto, M., Nazarudin, N., and Nandiyanto, A. B. D. (2022). Sustainable compost prepared from oyster mushroom substrate microparticles with domestic wastes as local starters. *Moroccan Journal of Chemistry, 10*(4), 726-737.

[20] Nandiyanto, A. B. D., Ragadhita, R., Girsang, G. C. S., Anggraeni, S., Putri, S. R., Sadiyyah, F. H., and Hibatulloh, M. R. (2022). Effect of palm fronds and rice husk composition ratio on the mechanical properties of composite-based brake pad. *Moroccan Journal of Chemistry*, *10*(4), 663-677.

[21] Rahmat, A., Ramadhani, W. S., Nur, M., Sutiharni, S., and Mutolib, A. (2022). Chemical properties of salacca seed biochar under low temperature of pyrolysis. *Applied Research in Science and Technology*, *2*(1), 43-46.

DOI: https://doi.org/10.17509/ajse.v5i1.81297
p- ISSN 2776-6098 e- ISSN 2776-5938

[22] Meziane, H., Laita, M., Azzaoui, K., Boulouiz, A., Neffa, M., Sabbahi, R., Nandiyanto, A. B. D., Elidrissi, A., Abidi, N., Siaj, M., and Touzani, R. (2024). Nanocellulose fibers: A review of preparation methods, characterization techniques, and reinforcement applications. *Moroccan Journal of Chemistry, 12*(1), 305-343.

[23] Nandiyanto, A. B. D., Putri, A. R., Pratiwi, V. A., Ilhami, V. I. N., Kaniawati, I., Kurniawan, T., Farobie, O., and Bilad, M. R. (2024). Fourier transform infrared spectroscopy (FTIR) of pyrolysis of polypropylene microparticles and its chemical reaction mechanism completed with computational bibliometric literature review to support sustainable development goals (SDGs). *Journal of Engineering Science and Technology, 19*(3), 1090-1104.

[24] Rahmat, A., Hidayat, H., Lestari, L. P., Elfarisna, E., Indriyani, I., Apriyanto, M., Nuraini, L., Hariadi, H., and Mutolib, A. (2024). Evaluation of the characteristics of avocado seed biochar at various pyrolysis temperatures for sustainable waste management. *Universal Journal of Agricultural Research, 12*(1), 201-210.

[25] Rahmat, A., Awwaliyah, A. S., Hidayat, H., Budiharto, I. W., Arum, F., Respati, S. A., Susanti, W. D., and Sukamto, S. (2024). Effect of pyrolysis temperature on the properties of biochar derived from melinjo seed shells. *International Journal of Heat and Technology, 42*(6), 1924-1934.

[26] Nandiyanto, A. B. D., Maryanti, R., Fiandini, M., Ragadhita, R., Usdiyana, D., Anggraeni, S., Arwa, W. R., and Al-Obaidi, A. S. M. (2020). Synthesis of carbon microparticles from red dragon fruit (*Hylocereus undatus*) peel waste and their adsorption isotherm characteristics. *Molekul, 15*(3), 199-209.

[27] N'diaye, A. D., Kankou, M. S., Hammouti, B., Nandiyanto, A. B. D., and Al Husaeni, D. F. (2022). A review of biomaterial as an adsorbent: From the bibliometric literature review, the definition of dyes and adsorbent, the adsorption phenomena and isotherm models, factors affecting the adsorption process, to the use of *Typha* species waste as a low-cost adsorbent. *Communications in Science and Technology, 7*(2), 140-153.

[28] Nandiyanto, A. B., Azizah, N. N., and Taufik, R. S. R. (2022). Investigation of adsorption performance of calcium carbonate microparticles prepared from eggshells waste. *Journal of Engineering Science and Technology, 17*(3), 1934-1943.

[29] Ragadhita, R., Amalliya, A., Nuryandi, S., Fiandini, M., Nandiyanto, A. B. D., Hufad, A., Mudzakir, A., Nugraha, W. C., Farobie, O., Istadi, I., and Al-Obaidi, A. S. M. (2023). Sustainable carbon-based biosorbent particles from papaya seed waste: Preparation and adsorption isotherm. *Moroccan Journal of Chemistry, 11*(2), 395-410.

[30] Ramdhani, M. R., Kholik, A., Fauziah, R. S. P., Roestamy, M., Suherman, I., and Nandiyanto, A. B. D. (2023). A comprehensive study on biochar production, bibliometric analysis, and collaborative teaching practicum for sustainable development goals (SDGs) in Islamic schools. *Jurnal Pendidikan Islam, 9*(2), 123-144.

[31] Nandiyanto, A. B. D., Fiandini, M., Ragadhita, R., Maryanti, R., Husaeni, D. F. A., and Husaeni, D. N. (2023). Removal of curcumin dyes from aqueous solutions using carbon microparticles from jackfruit seeds by batch adsorption experiment. *Journal of Engineering Science and Technology, 18*(1), 653-670.

DOI: https://doi.org/10.17509/ajse.v5i1.81297
p- ISSN 2775-6793 e- ISSN 2775-6815

[32] Nandiyanto, A. B. D., Ragadhita, R., Fiandini, M., Maryanti, R., Husaeni, D. N. A., and Husaeni, D. F. A. (2023). Adsorption isotherm characteristics of calcium carbon microparticles prepared from chicken bone waste to support sustainable development goals (SDGs). *Journal of Engineering Science and Technology, 18*(2), 1363-1379.

[33] Nandiyanto, A. B. D., Fiandini, M., Fadiah, D. A., Muktakin, P. A., Ragadhita, R., Nugraha, W. C., Kurniawan, T., Bilad, M. R., Yunas, J., and Al Obaidi, A. S. M. (2023). Sustainable biochar carbon microparticles based on mangosteen peel as biosorbent for dye removal: Theoretical review, modelling, and adsorption isotherm characteristics. *Journal of Advanced Research in Fluid Mechanics and Thermal Sciences, 105*(1), 41-58.

[34] Nandiyanto, A. B. D., Nugraha, W. C., Yustia, I., Ragadhita, R., Fiandini, M., Saleh, M., and Ningwulan, D. R. (2023). Rice husk for adsorbing dyes in wastewater: Literature review of agricultural waste adsorbent, preparation of rice husk particles, particle size on adsorption characteristics with mechanism and adsorption isotherm. *Journal of Advanced Research in Applied Mechanics, 106*(1), 1-13.

[35] Nandiyanto, A. B. D., Fiandini, M., Ragadhita, R., Maulani, H., Nurbaiti, M., Al-Obaidi, A. S. M., Yunas, J., and Bilad, M. R. (2023). Sustainable biochar carbon biosorbent based on tamarind (*Tamarindus indica* L.) seed: Literature review, preparation, and adsorption isotherm. *Journal of Advanced Research in Applied Sciences and Engineering Technology, 32*(1), 210-226.

[36] Nandiyanto, A. B. D., Fiandini, M., Ragadhita, R., and Aziz, M. (2023). How to purify and experiment with dye adsorption using carbon: Step-by-step procedure from carbon conversion from agricultural biomass to concentration measurement using UV-Vis spectroscopy. *Indonesian Journal of Science and Technology, 8*(3), 363-380.

[37] Nandiyanto, A. B. D., Nugraha, W. C., Yustia, I., Ragadhita, R., Fiandini, M., Meirinawati, H., and Wulan, D. R. (2024). Isotherm and kinetic adsorption of rice husk particles as a model adsorbent for solving issues in the sustainable gold mining environment from mercury leaching. *Journal of Mining Institute, 265*, 104-120.

[38] Nandiyanto, A. B. D., Putri, M. E., Fiandini, M., Ragadhita, R., Kurniawan, T., Farobie, O., and Bilad, M. R. (2024). Characteristics of ammonia adsorption on various sizes of calcium carbonate microparticles from chicken eggshell waste. *Moroccan Journal of Chemistry, 12*(3), 1073-1096.

[39] Nandiyanto, A. B. D., Fiandini, M., and Al Husaeni, D. N. (2024). Research trends from the Scopus database using keyword water hyacinth and ecosystem: A bibliometric literature review. *ASEAN Journal of Science and Engineering, 4*(1), 33-48.

[40] Nandiyanto, A. B. D., Ragadhita, R., Hofifah, S. N., Al Husaeni, D. F., Al Husaeni, D. N., Fiandini, M., Luckiardi, S., Soegoto, E. S., Darmawan, A., and Aziz, M. (2024). Progress in the utilization of water hyacinth as effective biomass material. *Environment, Development and Sustainability, 26*, 24521-24568.

[41] Mubarokah, S. L., Anwar, S., Nisa, K., Miftah, H., Hastuti, A., and Nandiyanto, A. B. D. (2024). Bibliometrics study on agro-economy of biochar. *Journal of Engineering Science and Technology*, *19,* 142-152.

DOI: https://doi.org/10.17509/ajse.v5i1.81297
p- ISSN 2776-6098 e- ISSN 2776-5938

[42] Martin, A. Y., Roestamy, M., Qolyubi, A. T., Hakim, A. L., and Nandiyanto, A. B. D. (2024). Bibliometric analysis of the use of biochar in an environmental law perspective. *Journal of Engineering Science and Technology, 19*, 167-176.

[43] Nandiyanto, A. B. D., Putri, A. E., Fiandini, M., Ragadhita, R., and Kurniawan, T. (2025). Biochar microparticles from pomegranate peel waste: Literature review and experiments in isotherm adsorption of ammonia. *Applied Science and Engineering Progress, 18*(1), 7506.

[44] Nandiyanto, A. B. D., Putri, N. R., Salimah, N. N., Al' Hafsah, S. H., Yunatraya, S. A., Fiandini, M., Bilad, M. R., Kurniawan, T., Gandidi, I. M., and Sukrawan, Y. (2025). Utilizing cassava peel-derived carbon biochar for ammonia adsorption to support hydrogen storage and sustainable development goals (SDGs): Effect of microparticle size and isothermal analysis. *Moroccan Journal of Chemistry, 13*(1), 424-439.

[45] Nandiyanto, A. B. D., Putri, N. R., Firdaus, N. N., Anzety, N. D., Al'Hafsah, S. H., Yunatraya, S. A., Fiandini, M., Bilad, M. R., Kurniawan, T., Gandidi, I. M., and Sukrawan, Y. (2025). Red onion peel biomass carbon microparticles for ammonia adsorption for supporting hydrogen storage and sustainable development goals (SDGs) with isotherm analysis. *Journal of Engineering Science and Technology, 20*(1), 181-194.

[46] Nandiyanto, A. B., Nugraha, A. Y., Fawwaz, L. T., Pramajati, M. F., Wijaya, Y. T., Fiandini, M., Bilad, M. R., Kurniawan, T., Gandidi, I. M., and Sukrawan, Y. (2025). Utilization of orange peel-derived biochar for ammonia adsorption: Isotherm analysis and hydrogen storage prospective for supporting sustainable development goals (SDGs). *Journal of Engineering Science and Technology, 20*(1), 85-98.

[47] Nandiyanto, A. B. D. (2020). Isotherm adsorption of carbon microparticles prepared from pumpkin (Cucurbita maxima) seeds using two-parameter monolayer adsorption models and equations. *Moroccan Journal of Chemistry*, *8*(3), 745-761.

[48] Nayaggy, M., and Putra, Z. A. (2019). Process simulation on fast pyrolysis of palm kernel shell for production of fuel. *Indonesian Journal of Science and Technology, 4*(1), 64-73.

[49] Subagyono, R. D. J., Qi, Y., Chaffee, A. L., Amirta, R., and Marshall, M. (2021). Pyrolysis-GC/MS analysis of fast growing wood Macaranga species. *Indonesian Journal of Science and Technology, 6*(1), 141-158.

[50] Jamilatun, S., Pitoyo, J., Amelia, S., Ma'arif, A., Hakika, D. C., and Mufandi, I. (2022). Experimental study on the characterization of pyrolysis products from bagasse (*Saccharum officinarum* L.): Bio-oil, biochar, and gas products. *Indonesian Journal of Science and Technology, 7*(3), 565-582.

[51] Jelita, R., Nata, I. F., Irawan, C., Jefriadi, J., Anisa, M. N., Mahdi, M. J., and Putra, M. D. (2023). Potential alternative energy of hybrid coal from co-pyrolysis of lignite with palm empty fruit bunch and the kinetic study. *Indonesian Journal of Science and Technology, 8*(1), 97-112.

[52] Mutolib, A., Rahmat, A., Triwisesa, E., Hidayat, H., Hariadi, H., Kurniawan, K., Sutiharni, S., and Sukamto, S. (2023). Biochar from agricultural waste for soil amendment candidate under different pyrolysis temperatures. *Indonesian Journal of Science and Technology, 8*(2), 243-258.

DOI: https://doi.org/10.17509/ajse.v5i1.81297
p- ISSN 2775-6793 e- ISSN 2775-6815

[53] Jamilatun, S., Aziz, M., and Pitoyo, J. (2023). Multi-distributed activation energy model for pyrolysis of sugarcane bagasse: Modelling strategy and thermodynamic characterization. *Indonesian Journal of Science and Technology, 8*(3), 413-428.

[54] Rahmat, A., Sutiharni, S., Elfina, Y., Yusnaini, Y., Latuponu, H., Minah, F. N., Sulistyowati, Y., and Mutolib, A. (2023). Characteristics of tamarind seed biochar at different pyrolysis temperatures as waste management strategy: Experiments and bibliometric analysis. *Indonesian Journal of Science and Technology, 8*(3), 517-538.

[55] Sridevi, V., Hamzah, H. T., Jweeg, M. J., Mohammed, M. N., Al-Zahiwat, M. M., Abdullah, T. A., and Abdullah, O. I. (2024). Microwave pyrolysis of agricultural and plastic wastes for production of hybrid biochar: Applications for greener environment. *Indonesian Journal of Science and Technology, 9*(3), 791-820.

[56] Pebrianti, M., and Salamah, F. (2021). Learning simple pyrolysis tools for turning plastic waste into fuel. *Indonesian Journal of Multidisciplinary Research, 1*(1), 99-102.

[57] Alhinai, M., Azad, A. K., Bakar, M. A., and Phusunti, N. (2018). Characterization and thermochemical conversion of rice husk for biochar production. *International Journal of Renewable Energy Research, 8*(3), 1648-1656.

[58] Tsai, W. T., Lee, M. K., and Chang, Y. M. (2007). Fast pyrolysis of rice husk: Product yields and compositions. *Bioresource Technology, 98*(1), 22-28.

[59] Prapagdee, S., Piyatiratitivorakul, S., and Petsom, A. (2016). Physico-chemical activation on rice husk biochar for enhancing cadmium removal from aqueous solution. *Asian Journal of Water, Environment and Pollution, 13*(1), 27-34.

[60] Antonangelo, J. A., Zhang, H., Sun, X., and Kumar, A. (2019). Physicochemical properties and morphology of biochars as affected by feedstock sources and pyrolysis temperatures. *Biochar, 1*, 325-336.

[61] Reza, M. S., Afroze, S., Bakar, M. S. A., Saidur, R., Aslfattahi, N., Taweekun, J., and Azad, A. K. (2020a). Biochar characterization of invasive *Pennisetum purpureum* grass: Effect of pyrolysis temperature. *Biochar, 2*, 239-251.

[62] Claoston, N., Samsuri, A. W., Husni, M. H. A., and Amran, M. S. M. (2014). Effects of pyrolysis temperature on the physicochemical properties of empty fruit bunch and rice husk biochars. *Waste Management and Research, 32*(4), 331-339.

[63] Cha, J. S., Park, S. H., Jung, S.-C., Ryu, C., Jeon, J.-K., Shin, M.-C., and Park, Y.-K. (2016). Production and utilization of biochar: A review. *Journal of Industrial and Engineering Chemistry, 40*, 1-15.

[64] Angın, D. (2013). Effect of pyrolysis temperature and heating rate on biochar obtained from pyrolysis of safflower seed press cake. *Bioresource Technology, 128*, 593-597.

[65] Ronsse, F., Van Hecke, S., Dickinson, D., and Prins, W. (2012). Production and characterization of slow pyrolysis biochar: Influence of feedstock type and pyrolysis conditions. *Global Change Biology Bioenergy, 5(2)*, 104-115.

[66] Ragadhita, R., and Nandiyanto, A. B. D. (2022). Why 200°C is effective for creating carbon from organic waste (from thermal gravity (TG-DTA) perspective)?. *ASEAN Journal for Science and Engineering in Materials, 2(2)*, 75-80.

DOI: https://doi.org/10.17509/ajse.v5i1.81297
p- ISSN 2776-6098 e- ISSN 2776-5938

[67] Nandiyanto, A. B. D. (2017). Mathematical approximation based on thermal analysis curves for calculating kinetic parameters of thermal decomposition of material. *Journal of Engineering Science and Technology, 12(5)*, 76-90.

[68] Yahya, M. A., Al-Qodah, Z., and Ngah, C. Z. (2015). Agricultural bio-waste materials as potential sustainable precursors used for activated carbon production: A review. *Renewable and Sustainable Energy Reviews, 46*, 218-235.

[69] Chen, B., Zhou, D., and Zhu, L. (2008). Transitional adsorption and partition of nonpolar and polar aromatic contaminants by biochars of pine needles with different pyrolytic temperatures. *Environmental Science and Technology, 42(14)*, 5137-5143.

[70] Yuan, J. H., Xu, R. K., and Zhang, H. (2011b). The forms of alkalis in the biochar produced from crop residues at different temperatures. *Bioresource Technology, 102*(3), 3488-3497.

[71] Demirbas, A. (2004). Effects of temperature and particle size on bio-char yield from pyrolysis of agricultural residues. *Journal of Analytical and Applied Pyrolysis, 72*(2), 243-248.

[72] Keiluweit, M., Nico, P. S., Johnson, M. G., and Kleber, M. (2010). Dynamic molecular structure of plant biomass-derived black carbon (biochar). *Environmental Science and Technology, 44*(4), 1247-1253.

[73] Irwansyah, F. S., Amal, A. I., Diyanthi, E. W., Hadisantoso, E. P., Noviyanti, A. R., Eddy, D. R., and Risdiana, R. (2024). How to read and determine the specific surface area of inorganic materials using the Brunauer-Emmett-Teller (BET) method. *ASEAN Journal of Science and Engineering, 4*(1), 61-70.

[74] Ahmad, M., Lee, S. S., Dou, X., Mohan, D., Sung, J. K., Yang, J. E., and Ok, Y. S. (2012). Effects of pyrolysis temperature on soybean stover and peanut shell-derived biochar properties and TCE adsorption in water. *Bioresource Technology, 118*, 536-544.

[75] Shaaban, A., Se, S. M., Dimin, M. F., Juoi, J. M., Husin, M. H., and Mitan, N. M. M. (2014). Influence of heating temperature and holding time on biochars derived from rubber wood sawdust via slow pyrolysis. *Journal of Analytical and Applied Pyrolysis, 107*, 31-39.

[76] Kavitha, B., Reddy, P. V. L., Kim, B., Lee, S. S., Pandey, S. K., and Kim, K. H. (2018). Benefits and limitations of biochar amendment in agricultural soils: A review. *Journal of Environmental Management, 227*, 146-154.

[77] Tan, I., Ahmad, A., and Hameed, B. (2008). Preparation of activated carbon from coconut husk: Optimization study on removal of 2,4,6-trichlorophenol using response surface methodology. *Journal of Hazardous Materials, 153*(1-2), 709-717.

[78] Wang, T., Liu, H., Duan, C., Xu, R., Zhang, Z., She, D., and Zheng, J. (2020). The eco-friendly biochar and valuable bio-oil from *Caragana korshinskii*: Pyrolysis preparation, characterization, and adsorption applications. *Materials, 13*(15), 1-20.

[79] Jiang, Y., Li, C., Zhang, L., Fan, M., Zhang, S., Gao, W., Li, B., Wang, S., and Hu, X. (2023). Pyrolysis of banana peel with microwave and furnace as the heating sources: The distinct impacts on evolution of the pyrolytic products. *Process Safety and Environmental Protection*, 173, 373-383.

DOI: https://doi.org/10.17509/ajse.v5i1.81297
p- ISSN 2775-6793 e- ISSN 2775-6815

[80] Jalalabadi, T., Wu, J., Moghtaderi, B., Sharma, N., and Allen, J. (2023). A new approach to turbostratic carbon production via thermal salt-assisted treatment of graphite. *Fuel, 348*, 128489.

[81] Pusceddu, E., Montanaro, A., Fioravanti, G., Santilli, S. F., Foscolo, P. U., Criscuoli, I., Raschi, A., and Miglietta, F. (2017). Comparison between ancient and fresh biochar samples: A study on the recalcitrance of carbonaceous structures during soil incubation. *International Journal of New Technology and Research, 3*(3), 39-46.

[82] Han, Y., Gholizadeh, M., Tran, C. C., Kaliaguine, S., Li, C. Z., Olarte, M., and Garcia-Perez, M. (2019). Hydrotreatment of pyrolysis bio-oil: A review. *Fuel Processing Technology, 195*, 106140.

[83] Paris, O., Loidl, D., Peterlik, H., Müller, M., Lichtenegger, H., and Fratzl, P. (2000). The internal structure of single carbon fibers determined by simultaneous small- and wide-angle X-ray scattering. *Journal of Applied Crystallography, 33*(3), 695-699.

[84] Nadarajah, K., Asharp, T., and Jeganathan, Y. (2024). Biochar from waste biomass, its fundamentals, engineering aspects, and potential applications: an overview. *Water Science and Technology, 89*(5), 1211-1239.

[85] Tomczyk, A., Sokołowska, Z., and Boguta, P. (2020). Biochar physicochemical properties: Pyrolysis temperature and feedstock kind effects. *Reviews in Environmental Science and Biotechnology, 19*(1), 191-215.

[86] Nandiyanto, A. B. D., Oktiani, R., and Ragadhita, R. (2019). How to read and interpret FTIR spectroscope of organic material. *Indonesian Journal of Science and Technology, 4*(1), 97-118.

[87] Nandiyanto, A. B. D., Ragadhita, R., and Fiandini, M. (2023). Interpretation of Fourier Transform Infrared Spectra (FTIR): A practical approach in the polymer/plastic thermal decomposition. *Indonesian Journal of Science and Technology, 8*(1), 113-126.

[88] Sukamto, S., and Rahmat, A. (2023). Evaluation of FTIR, macro and micronutrients of compost from black soldier fly residual: In context of its use as fertilizer. *ASEAN Journal of Science and Engineering, 3*(1), 21-30.

[89] Obinna, E. N. (2022). Physicochemical properties of human hair using Fourier Transform Infra-Red (FTIR) and Scanning Electron Microscope (SEM). *ASEAN Journal for Science and Engineering in Materials, 1*(2), 71-74.

[90] Chi, M., Xu, X., Cui, D., Zhang, H., and Wang, Q. (2016). A TG-FTIR investigation and kinetic analysis of oil shale kerogen pyrolysis using the distributed activation energy model. *Oil Shale, 33*(3), 228-247.

[91] Tahir, M. H., Zhao, Z., Ren, J., Rasool, T., and Naqvi, S. R. (2019). Thermo-kinetics and gaseous product analysis of banana peel pyrolysis for its bioenergy potential. *Biomass and Bioenergy, 122*, 193-201.

[92] Fildza, M., Rohmatullaili, R., and Oktasari, A. (2022). Utilization of Jengkol Peel (*Pithecellobium jiringa*) as an adsorbent of iron metal. *Walisongo Journal of Chemistry, 5(2)*, 130-135.

DOI: https://doi.org/10.17509/ajse.v5i1.81297
p- ISSN 2776-6098 e- ISSN 2776-5938

[93] Gonçalves Martins, J. P., Setter, C., Ataíde, C. H., Pires de Oliveira, T. J., and Magriotis, Z. M. (2021). Study of pequi peel pyrolysis: Thermal decomposition analysis and product characterization. *Biomass and Bioenergy, 149*, 106095.

[94] Abidi, S., Trabelsi, A. B. H., and Boudhrioua, N. (2023). Pyrolysis of lemon peel waste in a fixed-bed reactor and characterization of innovative pyrolytic products. *Journal of Material Cycles and Waste Management, 25*(1), 235-248.

[95] Park, J., Hung, I., Gan, Z., Rojas, O. J., Lim, K. H., and Park, S. (2013). Activated carbon from biochar: Influence of its physicochemical properties on the sorption characteristics of phenanthrene. *Bioresource Technology, 149*, 383-389.

[96] Iskandar, T., and Rofiatin, U. (2017). Karakteristik biochar berdasarkan jenis biomassa dan parameter proses pirolisis. *Jurnal Teknik Kimia, 12*(1), 28-35.

[97] Puspita, V., Syakur, S., and Darusman, D. (2021). Karakteristik biochar sekam padi pada dua temperatur pirolisis. *Jurnal Ilmiah Mahasiswa Pertanian, 6*(4), 732-739.

[98] Pratiwi, D., Syakur, S., and Darusman, D. (2021). Karakteristik biochar pada beberapa metode pembuatan dan bahan baku. *Jurnal Ilmiah Mahasiswa Pertanian, 6*(3), 210-216.

[99] Enders, A., Hanley, K., Whitman, T., Joseph, S., and Lehmann, J. (2012). Characterization of biochars to evaluate recalcitrance and agronomic performance. *Bioresource Technology, 114*, 644-653.

[100] Uchimiya, M., Wartelle, L. H., Klasson, K. T., Fortier, C. A., and Lima, I. M. (2011). Influence of pyrolysis temperature on biochar property and function as a heavy metal sorbent in soil. *Journal of Agricultural and Food Chemistry, 59(6)*, 2501-2510.

[101] Soedarmanto, H., Setiawaty, E., and Iskandar, T. (2021). Optimasi kadar ultimate dan tingkat kebasaan bio-arang limbah kayu durian sebagai pembenah tanah. *Jurnal Selulosa, 11(2)*, 59-68.

[102] Cantrell, K. B., Hunt, P. G., Uchimiya, M., Novak, J. M., and Ro, K. S. (2012). Impact of pyrolysis temperature and manure source on physicochemical characteristics of biochar. *Bioresource Technology, 107*, 419-428.

[103] Al Falaq, F., Juanda, B. R., and Siregar, D. S. (2020). Respon pertumbuhan dan hasil tanaman terung (*Solanum melongena* L.) terhadap dosis pupuk organik cair GDM dan pupuk organik padat. *Jurnal Agrosamudra, 7*(2), 1-13.

[104] Lisdiyanti, M., and Guchi, H. (2018). Pengaruh pemberian bahan humat dan pupuk SP-36 untuk meningkatkan ketersediaan fosfor pada tanah ultisol. *Jurnal Pertanian Tropik, 5*(2), 192-198.

[105] Widowati, W., Asnah, A., and Sutoyo, S. (2012). Pengaruh penggunaan biochar dan pupuk kalium terhadap pencucian dan serapan kalium pada tanaman jagung. *Buana Sains, 12*(1), 83-90.

[106] Al Mu'min, M. I., Joy, B., and Yuniarti, A. (2016). Dinamika kalium tanah dan hasil padi sawah (*Oryza sativa* L.) akibat pemberian NPK majemuk dan penggenangan pada *Fluvaquentic Epiaquepts*. *Soilrens, 14*(1), 11-15.

[107] Gunes, A., Inal, A., Sahin, O., Taskin, M. B., Atakol, O., and Yilmaz, N. (2015). Variations in mineral element concentrations of poultry manure biochar obtained at different

DOI: https://doi.org/10.17509/ajse.v5i1.81297
p- ISSN 2775-6793 e- ISSN 2775-6815

pyrolysis temperatures, and their effects on crop growth and mineral nutrition. *Soil Use and Management, 31(4),* 429-437.

[108] Aryandhita, M. I., and Kastono, D. (2021). Pengaruh pupuk kalsium dan kalium terhadap pertumbuhan dan kualitas hasil sawi hijau (*Brassica rapa* L.). *Vegetalika, 10(2),* 107-119.

[109] Rosmiah, R., Aminah, R. I. S., Astuti, D. T., Marlina, N., Meidalima, D., and Pratama, B. (2023). Utilization of jengkol (*Pithecellobium jiringa*) peel biochar and chicken manure as organic fertilizer on red chili plants (*Capsicum annum* L.) in acidic dry land. *Jurnal Lahan Suboptimal: Journal of Suboptimal Lands, 12*(2), 129-138.

[110] Chettri, D., Boro, D., Chirania, M., and Verma, A. K. (2024). Integrating biochar production in biorefineries: Towards a sustainable future and circular economy. *Biofuels, Bioproducts and Biorefining, 18*(6), 2156-2176.

[111] Prochnow, F. D., Cavali, M., Dresch, A. P., Belli, I. M., Libardi, N. J., and de Castilhos, A. B. J. (2024). Biochar: From laboratory to industry scale—An overview of scientific and industrial advances, opportunities in the Brazilian context, and contributions to sustainable development. *Processes, 12*, 1006.

DOI: https://doi.org/10.17509/ajse.v5i1.81297
p- ISSN 2776-6098 e- ISSN 2776-5938